Title

E-cigarettes and Western Diet: Important Metabolic Risk Factors for Hepatic Diseases



Journal

Hepatology, 69(6)

ISSN

0270-9139

Authors

Hasan, Kamrul M

Friedman, Theodore C

Shao, Xuesi

et al.

Publication Date

2019-06-01

DOI

10.1002/hep.30512

Peer reviewed

HHS Public Access

Author manuscript

*Hepatology*. Author manuscript; available in PMC 2019 July 17.

Published in final edited form as:

*Hepatology*. 2019 June ; 69(6): 2442–2454. doi:10.1002/hep.30512.

# E-cigarettes and Western Diet: Important Metabolic Risk Factors for Hepatic Diseases

**Kamrul M. Hasan**[1], **Theodore C Friedman**[1,2], **Xuesi Shao**[1,2], **Meher Parveen**[1], **Carl Sims**[1], **Desean L. Lee**[1], **Jorge Espinoza-Derout**[1], **Indrani Sinha-Hikim**[1,2], and **Amiya P. Sinha-Hikim**[1,2]

[1]Division of Endocrinology, Metabolism and Molecular Medicine, Department of Internal Medicine, Charles R. Drew University, Los Angeles, CA 90059,

[2]David Geffen School of Medicine at University of California, Los Angeles, Los Angeles, CA 90095.

## Abstract

The use of electronic nicotine delivery systems (ENDS), also known as e-cigarettes, with a variety of e-liquids/e-juices, is increasing at an alarming rate among adolescents who do not realize their potential harmful health effects. This study examines the harmful effects of ENDS on the liver. Apolipoprotein E null (ApoE−/−) mice on a western diet (WD) were exposed to saline or ENDS with 2.4% nicotine aerosol for 12 weeks using our newly developed mouse ENDS exposure model system that delivers nicotine to mice that leads to equivalent serum cotinine levels found in human cigarette users. ApoE−/− mice on a WD exposed to ENDS exhibited a marked increase in hepatic lipid accumulation compared to ApoE−/− on a similar diet exposed to saline aerosol. The detrimental effects of ENDS on hepatic steatosis were associated with significantly greater oxidative stress, increased hepatic triglyceride levels and increased hepatocyte apoptosis, independent of AMP-activated protein kinase (AMPK) signaling. In addition, hepatic RNA seq analysis revealed that 433 genes were differentially expressed in ENDS-exposed mice on WD compared to saline-exposed mice. Functional analysis indicates that genes associated with lipid metabolism, cholesterol biosynthesis, and circadian rhythm were most significantly altered in the liver in response to ENDS. These results demonstrate profound adverse effects of ENDS on the liver. This is important information for regulatory agencies as they regulate ENDS.

### Keywords

E-cigarette; nicotine; oxidative stress; apoptosis; hepatic steatosis; lipogenesis; Circadian system; NAFLD; RNA seq

**Address for Correspondence:** Kamrul M. Hasan, Ph.D. Division of Endocrinology, Metabolism and Molecular Medicine, Department of Internal Medicine, Charles R. Drew University of Medicine and Science, 1731 E. 120th Street, Los Angeles, CA 90059. Tel: 323563-5974, Fax: 323-563-9352, kamrulhasan@cdrewu.edu.

Disclosure statement: The authors have nothing to disclose.

## Introduction

Electronic nicotine delivery systems (ENDS), also known as e-cigarettes, are battery powered inhalation devices designed to deliver nicotine to users without burning tobacco. ENDS are rapidly gaining popularity and, thus, have drawn attention from lawmakers, health organizations, researchers, smokers and non-smokers (1). As their popularity have increased, e-cigarettes have become the subject of a public health disputes as some experts welcome them as a pathway to the reduction or cessation of tobacco use, while opponents characterize them as a dangerous product that could undermine efforts to de-normalize smoking (2). What is more frightening is that an earlier cross sectional analysis of survey data from a representative sample of middle and high school students in 2011 (n=17,353) and 2012 (n=22,529) suggests that ENDS may contribute to nicotine addiction and are unlikely to discourage conventional cigarette smoking among youths (3), indicating that ENDS could generate a new market for nicotine dependence. Recent studies also consistently reveal that most people who use ENDS are so-called dual users, meaning that they use ENDS as well as conventional cigarettes (4–6). Furthermore, an increasing number of both in vivo and in vitro studies reporting a range of adverse effects of e-cigarettes or e-juices exposure in cell/organ systems, including lung (7), liver (8, 9), and the cardiovascular system. A recent cross-sectional case control study of habitual e-cigarette users (n=23) and non-user control individuals (n=19) showed increased cardiac sympathetic activity and oxidative stress, both associated with increased cardiovascular risk, in habitual e-cigarette users (10). As ENDS are a relatively new product, studies are needed to determine their long-term detrimental effects, some of which may be similar to the long-term detrimental effects of nicotine.

In earlier studies, we demonstrated that twice daily intraperitoneal (IP) injections of nicotine (0.75 mg/kg BW) when combined with a high-fat diet (HFD) triggers greater oxidative stress, activates hepatocyte apoptosis, and amplifies hepatic steatosis (11, 12). The additive effects of nicotine and HFD on the severity of hepatic steatosis were further associated with inactivation of AMP-activated protein kinase (AMPK) and activation of its downstream target acetyl-COA carboxylase (ACC), leading to stimulation of lipogenesis (11, 12). The objectives of the present study are 2-fold. The first is to examine whether ENDS exposure can exacerbate hepatic steatosis in apolipoprotein E null (ApoE−/−) mice on a WD. The second is to examine whether the same AMPK-mediated pathway is also the key pathway for induction of hepatic steatosis. We elected to use ApoE−/− mice, as these animals, when fed a WD with 45% fat, as opposed to a very HFD with 60% of calories derived from fat develop hepatic steatosis (13). These mice on a WD represent a novel and fast model with all characteristics feature of nonalcoholic steatohepatitis (NASH) and metabolic syndrome, including abnormal glucose tolerance, hepatomegaly, hepatic steatosis, liver fibrosis and inflammation (14). Furthermore, because nonalcoholic fatty liver disease (NAFLD) has been identified as an independent risk factor of atherosclerosis and cardiovascular disease (15, 16), an additional advantage of this model is that it is an ideal model for linking atherosclerosis and NAFLD.

## Materials and Methods

### ANIMALS.

Adult (8 weeks old), male ApoE$^{-/-}$ mice on a C57BL/6J background were purchased from Jackson Laboratories (Bar Harbor, ME). Mice were housed under controlled temperature (22°C) and photoperiod (12-h light and 12-h dark cycle) with free access to water and food. Mice on a WD containing 0.21% cholesterol, 21% of calories from fat, 50% calories from carbohydrate, and 20% of calories from protein (D12079B; Research Diets, New Brunswick, NJ). They were exposed to ENDS or saline aerosol for 12 weeks using our ENDS aerosol generation and rodent exposure system (patent number PCT/US17/54133). As an additional control, we used Gold leaf tobacco (otherwise identical to Classic Tobacco) with 0% nicotine to differentiate whether our findings are due to the nicotine in the ENDS or to the vaporization of other non-nicotine ENDS ingredients.

We used a charged blu PLUS E-cigarette tank containing 2.4% nicotine of classic tobacco flavor. This system contains air pressure and flow rate control as well as hardware and software that allow experimenters to control the timing, duration and times/day for ENDS aerosol generation/exposure and can hold up to 5 mice. To deliver chronic intermittent ENDS, the device was activated for 4 sec per puff, 8 puffs per vaping episode with an inter-puff interval of 25 sec; one vaping episode every 30 min. Mice were exposed to intermittent ENDS (2.4%) or saline aerosol (17) (Afasci Inc, Burlingame, CA) for 12h (2100–0900). During the light phase of 12 h (0900 to 2100), mice were returned to their home cage and no aerosol was delivered. Animal handling and experimentation were in accordance with the recommendation of the American Veterinary Medical Association and were approved by the Charles R. Drew University School of Medicine and Science Institutional Animal Care and Use Committee (IACUC). Mice were fasted overnight before euthanasia with isoflurane. Livers were removed and portions of livers were placed in RNAIater and used for gene expression analysis by quantitative RT-PCR or snap frozen in liquid $N_2$ and stored frozen for RNA sequencing (RNASeq) analysis and subsequent measurements of triglycerides, oxidative stress, and changes in protein expression by immunoblotting. The remaining portions of liver were either fixed in 2.5% glutaraldehyde for high-resolution light and electron microscopy or 10% formalin for routine histological, immunohistochemical and immunofluorescence studies.

### LIVER PATHOLOGY.

Liver pathology was evaluated using conventional histological analysis on hematoxylin and eosin (H & E) stained sections. Further evaluation of pathology was achieved by high-resolution light microscopy using glutaraldehyde-fixed, osmium tetroxide post-fixed, epoxy-embedded, and toluidine blue-stained sections (11, 13) and electron microscopy. Liver fibrosis was evaluated by Sirius red staining of formalin-fixed, paraffin-embedded liver sections for visualization of collagen. Accumulation of intrahepatic fat and collagen content was quantified by computerized densitometry using the ImagePro Plus software (11–13). Further evaluation of liver fibrosis was assessed by measuring transforming growth factor alpha (TGF- α) and beta (TGF- β) (18, 19) by quantitative RT-PCR.

For electron microscopic studies, thin sections from selected tissue blocks were sectioned with an LKB ultramichrotome, stained with uranyl acetate, and examined with a Hitachi 600 electron microscope (Hitachi, Indianapolis, USA), as described before (11, 13).

## RNA SEQUENCING (RNA -seq) ANALYSIS.

Total RNA extracted from livers were sent to UCLA Technology Center for Genomics and Bioinformatics core for RNA seq analysis. RNA integrity was confirmed by using Bioanalyzer 2100 (Agilent Technologies, Santa Clara, CA, USA). Libraries for RNA-Seq were prepared with KAPA Stranded RNA-Seq Kit. Differentially expressed genes were identified using the edgeR program. Genes showing altered expression with $p < 0.05$ and >1.5 fold changes were considered differentially expressed. The pathway and network analyses were performed using Ingenuity Pathway Analysis software (IPA). IPA computes a score for each network according to the fit of the set of supplied focus genes. These scores indicate the likelihood of focused genes to belong to a network versus those obtained by chance. A score > 2 indicates a <99% confidence that a focus gene network was not generated by chance alone. The canonical pathways generated by IPA are the most significant for the uploaded data set. Fischer's exact test with FDR option was used to calculate the significance of the canonical pathway. For detailed methods, see supporting information)

## QUANTITATIVE RT-PCR.

Primers sequences were shown in supplementary Table 3. For detailed methods, see supporting information.

## WESTERN BLOTTING.

Western blotting was performed using liver lysates as described previously (11–13) using rabbit polyclonal phospho-AMPK (1:1000), total AMPK (1 : 1000), sterol regulatory element binding protein lc (SREBP1c), fatty acid synthase (FAS), phospho-ACC (1 : 1000), total ACC, cleaved caspase 9 (1 : 1 000), cleaved caspase 3 (1 : 1 000), cytochrome P450 family 4 subfamily a polypeptide A (CYP4A10; 1: 500), lipocalin 2 (LCN2; 1 :500), and B cell specific brain and muscle aryl hydrocarbon receptor translocator-like protein 1 (BMLI; 1:1000) antibodies for overnight at 4°C with constant shaking. GAPDH was used as loading control and was monitored using anti GAPDH antibody (1 : 5000). Band intensities were determined using Quantity One software from Bio-Rad.

Methods for measurements of cotinine levels, hepatic triglyceride levels, assessment of apoptosis and caspase activation, and hepatic oxidative stress are described in the Supporting Information.

## STATISTICAL ANALYSIS.

Animal experimentation was performed with 6 animals per group and data were presented as mean ± SEM. We used students T-test and Analysis of Variance (ANOVA) to assess the statistically significant differences among various treatment groups. If overall ANOVA revealed significant differences, post-hoc (pairwise) comparisons were performed using

Tukey's tests. Differences were considered significant if $P < 0.05$. Statistical analyses were performed using GraphPad Prism 5 (GraphPad Software, Inc., San Diego, CA).

## Results

### PLASMA COTININE LEVELS.

After 12 weeks of treatment, the concentration of plasma cotinine was 611 ± 54 ng/mL, that is in the range of heavy smokers who had smoked at least 18 cigarettes a day (20). In contrast, the concentration of plasma cotinine in mice that received saline and ENDS (0%) was undetectable.

### NICOTINE DELIVERED THROUGH ENDS TRIGGER GREATER OXIDATIVE STRESS AND CAUSE LIPID ACCUMULATION IN THE LIVER.

H & E-stained liver sections from ApoE−/− mice fed WD exposed to ENDS exhibited a marked increase in hepatic lipid accumulation than Apo E−/− mice on a similar diet exposed to saline aerosol (Fig. 1 A and B). These results were confirmed by high-resolution light microscopy; using glutaraldehyde-fixed, osmium tetroxide post-fixed, epoxy-embedded, and toluidine blue-stained liver sections (Fig. 1 C and D). ENDS exposure caused a striking increase in larger lipid droplets compared to those from mice exposed to saline. Quantitative image analysis further revealed a significant ($P<0.01$) increase in intracellular lipid content in mice exposed to ENDS ($179\pm10.2\mu m^2$) compared to mice exposed to saline aerosol ($37\pm2.3\mu m^2$).

We did not find progression of liver pathology, including infiltration of inflammatory cells, inflammatory foci, and portal/lobular fibrosis beyond steatosis of ENDS-treated mice. H&E stained liver sections from ApoE−/− mice on a WD exposed to ENDS with 0% nicotine exhibited little or no hepatic lipid accumulation and were comparable to that seen in mice exposed to saline aerosol (Supplementary Fig. 1). This is consistent with our recent studies indicating that it is only ENDS with nicotine and not without nicotine had pronounced adverse effects on cardiovascular structure and function (Espinoza-Derout J et al, manuscript submitted).

To further substantiate the light microscopic findings, we performed electron microscopic analysis (Fig. 1 E–H). Hepatocytes from ApoE−/− mice exposed to saline exhibited normal ultrastructure with abundant mitochondria and minimal lipid accumulation (Fig. 1E). In contrast, ENDS exposure led to a striking increase in lipid accumulation of varying sizes in hepatocytes along with a decrease in the amount of cellular organelles in ApoE−/−compared with those from mice exposed to saline (Fig. 1 F–H). A distinct increase in the incidence of hepatocyte apoptosis, characterized by nuclear condensation and fragmentation, and mitochondrial vacuolization was also noted in these mice following ENDS exposure (Fig. 1 H).

Compared to saline-treated mice, mice exposed to ENDS aerosol had significantly higher hepatic triglyceride levels (Fig. 1l). To test whether ENDS caused greater hepatic oxidative stress, we compared the in vivo expression of a lipid peroxidation product, 4-hydroxytrans-2-nonenal (4-HNE), a biomarker of oxidative stress (21). As shown in Fig. 1 J,

western blot analysis revealed significantly higher hepatic 4-HNE levels in ENDS-treated mice compared to saline-treated mice (Fig. 1 K). We also visualized 4-HNE expression by immunohistochemistry. Compared to saline-treated mice, mice exposed to ENDS aerosol had significantly higher 4-HNE immunoreactivity (Fig. 1 K).

## ENDS TRIGGER HEPATOCELLULAR APOPTOSIS AND ACTIVATE CASPASE 9 AND 3.

We next analyzed the incidence of apoptosis, expressed as percentage of TUNEL — positive nuclei per total nuclei (apoptotic plus non-apoptotic nuclei). Minimal hepatocyte apoptosis was noted in mice exposed to saline aerosol (Fig. 2A and B). In contrast, ENDS-exposed livers had significantly increased hepatocellular apoptosis by 2.0-fold over the values measured in saline-exposed liver (Fig 2A and B). To further substantiate this observation, we performed western blot analysis of the active (cleaved) initiator caspase 9 and active (cleaved) caspase 3 (Fig. 2C). Densitometric analysis revealed a significant increase in the hepatic expression of both active caspase 9 and caspase 3 of ENDS treated mice compared to controls (Fig. 2D and E).

## FIBROSIS.

We found no significant changes in the hepatic collagen deposition, as visualized by Sirius-Red staining, between saline and ENDS exposed livers in the presence or absence of nicotine (Supplementary Fig. 2 A and B). No significant changes in the expression of TGF-α and TGF-β, as revealed by both qRT-PCR (Supplementary Fig. 2 C) and RNA-seq analyses (Supplementary Fig. 2 D) were noted between saline and ENDS with nicotine exposed livers.

## AMPK-SREBP1c SIGNALING MAY BE DISPENSABLE FOR ENDS-INDUCED HEPATIC STEATOSIS.

AMPK, a central molecule of fatty acid metabolism (22) and plays a pivotal role in nicotine plus HFD-induced hepatic steatosis (11, 12). To investigate whether exacerbation of hepatic steatosis in mice exposed to ENDS is associated with inactivation (dephosphorylation) of AMPK, we carried out western blot analysis to test the phosphorylation status of the AMPK. Surprisingly, hepatic expression of phospho-AMPK was similar between control and ENDS treated livers (Fig. 3 A and B). Consistent with findings of no changes in the phosphorylation status of the AMPK in ENDS exposed liver, we found no significant changes in the hepatic expression of SREBP1c, FAS and phospho-ACC (Fig. 3 A and B).

We also monitored the hepatic expression of SREBP1c, FAS, peroxisome proliferator-activated receptor δ (PPAR δ), and insulin-induced gene 1 (INSIG1) by qRT-PCR. PPAR δ inhibits diet-induced hepatic steatosis by inducing the expression of INSIG which inhibits the SREBP1c (23). Consistent with our western blot data, no significant changes in the expression of these genes were noted between ENDS and saline aerosol exposed livers (Fig. 3 A and B).

## ENDS CAUSES HEPATIC STEATOSIS THROUGH PERTURBATION OF HEPATIC CHOLESTEROL AND LIPID METABOLISM, INFLAMMATION AND CIRCADIAN SYSTEMS ASSOCIATED NETWORKS.

To determine the molecular mechanisms by which ENDS exposure caused hepatic steatosis, we carried out RNA-sequencing (seq) analysis. Differentially expressed genes were identified through analysis of transcriptome sequencing data. Figure 4 A and B depict the two-dimensional hierarchical clustering of 433 differentially ($P<0.05$) expressed genes (for full list of genes, see supplemental Table 1 and 2). Each column represents one mouse and each row a gene probe set. Probe set signal values were normalized to the mean across the animals and the relative level of gene expression is depicted from the most down-regulated gene (green) to the most up-regulated gene (red), according to the scale shown on left. Of the 433 genes found to be differentially expressed in ENDS (2.4%) treated livers, 185 (42.72%) were up-regulated (for full list, see Supplementary Table 1) and 248 (57.28%) were down-regulated (for full list, see Supplementary Table 2). The RNA-seq analysis using IPA software, identified dysregulation of significant networks, canonical pathways and functions in ENDS treated livers in comparison to control livers (Fig.4 C and D). Among many other pathways, striking dysregulation of hepatic lipid metabolism and genes associated with cholesterol biosynthesis was over represented in the ENDS treated livers (Fig. 4 C). Similarly in terms of function and disease analysis, genes playing a key role in lipid metabolism and metabolic syndromes, among others, were significantly altered in the ENDS exposed livers (Fig. 4 D).

To validate the results of the genome-wide analysis, we performed quantitative RT-PCR on a set of genes regulated by ENDS (2.4%) identified using RNA-seq. As shown in Fig. 5A, quantitative RT-PCR data revealed significant up-regulation of Cyp4A10, Cyp2A4, and Cyp46 A1 and a significant down-regulation of lipocalin 2 (LCN2). There was no significant change in the expression of ACSL3 as revealed by both qRT-PCR and western blot analysis (Fig. 5 A–C). However, up-regulation of Cyp4A10 and down-regulation of LCN2 in the ENDS-treated livers were further substantiated by western blot analysis (Fig.5 B, D, E). As summarized in Table 1 , additional genes associated with the triglyceride synthesis and storage that were differentially expressed in ENDS-treated liver included up-regulation of monoacylglycero O-acyltransferase 1 (I MOGAT1), a gene linked with incorporation of fatty acid into triglyceride synthesis (24), cell death-inducing DNA fragmentation factor-alpha (DFFA)-Iike effector a (CIDEA) cell death inducing DFFA like effector c (CIDEC), genes involved with lipid storage and droplet formation (25). Besides excessive fat storage, another important feature of NAFLD is inflammation which causes hepatic injury. Though, we did not observe the induction of classic macrophage marker F4/80 (EMRI) in the liver following ENDS exposure, the expression of its related gene, EMR4 (26) , was significantly increased in the ENDS-treated mice. These changes were validated by quantitative RT-PCR. Taken together, these results indicate that ENDS can alter lipid metabolism through different mechanisms independent of AMPK signaling that favor ectopic lipid accumulation in the liver.

Intriguingly, our RNA seq analysis of hepatic transcriptome showed that expression of three prominent genes of the hepatic circadian core system, including BMAL1, neuronal PAS

domain protein 2 (NPAS2), and nuclear receptor subfamily 0 group B member 2 (NROB2) were down-regulated in ENDS-treated livers compared with saline-exposed livers (Fig. 6 A). Quantitative RT-PCR analysis also clearly showed that expression of these three genes were significantly down-regulated (Fig. 6 B) in the liver of mice exposed to ENDS. Hepatic downregulation of BMALI was further substantiated by western blot analysis (Fig.6 C and D).

## Discussion

In earlier studies using a model of diet-induced obesity, we demonstrated that nicotine (administered intraperitoneally) when combined with a HFD triggers greater oxidative stress, activates hepatocyte apoptosis, and exacerbates HFD-induced hepatic steatosis in C57BL6J mice compared to saline-treated mice. In this study, using a mouse model of NAFLD (13, 14), we elucidated some of the molecular mechanisms by which e-cigarettes or ENDS cause hepatic steatosis. The results of the present study provide evidence that: 1) nicotine delivered though ENDS causes hepatic steatosis, 2) AMPK-SREBP1c signaling is not required for ENDS-induced hepatic steatosis, and 3) ENDS-induced hepatic steatosis is mediated by increased oxidative stress and hepatocellular apoptosis together with perturbation of cholesterol and lipid metabolism and hepatic circadian system networks.

Oxidative stress coupled with hepatocyte apoptosis plays a pivotal role in the pathogenesis of NAFLD (27, 28). This study showed that compared to saline, ENDS generated greater oxidative stress. This is consistent with previous data showing that nicotine is capable of generating oxidative stress in various tissues including liver (29). Oxidative stress has also been implicated in apoptotic signaling in various cell types, including hepatocytes (30, 31). Thus, it is likely that generation of oxidative stress by ENDS triggers hepatocyte apoptosis and aggravate liver lesions through formation of the reactive and biologically active lipid peroxidation products such as 4-HNE. The observed increase in hepatic 4-HNE levels in ENDS exposed mice is consistent with this view. It is worth noting that a recent cross-sectional case control study showed increased cardiac sympathetic activity and oxidative stress in habitual e-cigarette users compared to non-user control individuals (10).

AMPK is a central regulator of lipid homeostasis and mediates suppression of lipogenic gene expression such as ACC and FAS through inhibition of SREBP1-c (37). Indeed in earlier studies (11, 12), we reported that inactivation of AMPK is critical for nicotine-induced hepatic steatosis in diet-induced obese C57BL/6 mice. However, unlike our earlier studies, here we found that AMPK-SREBP1c signaling is not required for ENDS-induced hepatic steatosis in ApoE−/− mice. The possible explanation of this difference is uncertain and cannot be explained by differences in animal models, but could depend on the duration of treatment or to the delivery of nicotine via ENDS. For example, ApoE−/− mice fed WD for 16 weeks do develop hepatic steatosis through inhibition of AMPK (13). There have also been studies showing that ApoB100 transgenic mice exposed to second-hand smoke for 19 weeks develop hepatic steatosis through inactivation of AMPK and activation of ACC (32). This clearly merits further investigation.

Steatosis, the hallmark feature of NAFLD, can occur as a result of excess free fatty acid (FAA) delivery from lipolysis of adipose tissue, increased *de novo* lipogenesis, and reduced fat oxidation and export in the form of very low-density lipoprotein (VLDL) (22, 33). We and others previously found that FFA derived from adipose tissue lipolysis plays a major role for hepatic triglycerides accumulation (27, 34). It is worth noting that nicotine has a direct effect on stimulating lipolysis in adipocytes (35, 36) which express nicotinic acetylcholine receptors (36, 37). These results, together with our previous findings that nicotine induces hepatic triglyceride accumulation through adipose tissue lipolysis in mice and that can be prevented by acipimox, an inhibitor of lipolysis (11), suggest that a similar mechanism is also responsible for ENDS-induced hepatic steatosis. However, we cannot rule out the possibility that in addition to increased FFA influx, other factors may have contributed to hepatic steatosis caused by ENDS exposure.

Intriguingly, our RNA seq analysis of hepatic transcriptome as well as quantitative RTPCR analysis showed that expression of three prominent genes of hepatic circadian core system such as BMAL1, NPAS2, and NR0B2 were down-regulated in ENDS-treated livers compared with saline-exposed livers. Hepatic down-regulation of BMAL1 in ENDS-treated mice was also substantiated by western blot analysis. Liver-specific knockout of BMAL1 increases hepatic oxidative stress and causes hepatic steatosis and insulin resistance (38, 39). It has been reported that primary dysregulated pathways in Npas2 −/− mice uniformly converge on hepatic lipid metabolism (40). NPAS2 and its small heterodimer partner (SHP or NR0B2) make a feedback loop controlling the expression of each other and their interplay controls hepatic lipid homeostasis (41). Dysregulation of NPAS2 has been noted in alcohol-induced hepatic steatosis (42).

One potential limitation of our study is that we used an ENDS delivery protocol that led to high (but still seen in human smokers) serum cotinine levels. Thus, it is possible that the observed detrimental effects of ENDS that are so obvious in this high delivery model might not be so obvious if given in lower dosages. In this context, it is worth noting here that in an ongoing study (Hasan K, unpublished data), we tested the detrimental effects of medium doses, generated form a dose-response study, of ENDS on the liver of C57BL6 male mice on a HFD, a commonly used model of diet-induced obesity. After 12 weeks of treatment, the concentrations of plasma nicotine and cotinine were 23.4 ± 3.3 and 254.1 ± 42.1 (mean ± SEM; ng/ml), respectively. These values are similar to the clinically relevant concentrations found in habitual smokers with nicotine levels ranging from 10–40 ng/ml and cotinine levels ranging from 100–300 ng/ml (43, 44). Intriguingly, HFD-fed mice exposed to a medium doses of ENDS also caused oxidative stress and hepatic steatosis compared to mice on a similar diet exposed to saline aerosol or ENDS with no nicotine.

In summary, we provided insights into the molecular mechanisms by which ENDS cause hepatic steatosis in a mouse model of NAFLD. Our findings question the popular belief that ENDS are safe and highlight multiple detrimental effects of ENDS on the liver. ENDS-induced hepatic steatosis is mediated by multiple mechanisms involving generation of oxidative stress and hepatocyte apoptosis, excess FFA delivery (possibly through adipose tissue lipolysis) and perturbations of cholesterol and lipid metabolism and hepatic circadian system networks.

## Supplementary Material

Refer to Web version on PubMed Central for supplementary material.

## Acknowledgments

This work was supported by the Diversity-Promoting Institution Drug Abuse Research Program (DIDARP) grant (R24DA017298), the Accelerating Excellence in Translational Science (AXIS) grant (2U54MD007598) from the National Institutes of Health (NIH) and California Tobacco-Related Disease Research Program (TRDRP) Grant 251P003.

## Abbreviations:

| | |
|---|---|
| **ACC** | Acetyl-COA-carboxylase |
| **AMPK** | Adenosine-5-monophosphate (AMP)-activated protein kinase |
| **ApoE** | Apolipoprotein E |
| **BMAL1** | B cell specific brain and muscle aryl hydrocarbon receptor translocator-like protein 1 |
| **CYP450** | Cytochrome P450 family of protein |
| **ENDS** | Electronic nicotine delivery systems |
| **FAS** | Fatty acid synthase |
| **4-HNE** | 4-hydroxy-trans-2-nonenal |
| **NAFLD** | Nonalcoholic fatty liver disease |
| **SREBP1c** | Sterol regulatory element binding protein 1c |

## REFERENCES

1. Hiemstra PS, Bals R. Basic science of electronic cigarettes: assessment in cell culture and in vivo models. Respir Res 2016; 17:127. [PubMed: 27717371]
2. Fairchild AL, Bayer R, Colgrove J. The renormalization of smoking? E-cigarettes and the tobacco “endgame”. N Engl J Med 2014;370:293–295. [PubMed: 24350902]
3. Dutra LM, Glantz SA. Electronic cigarettes and conventional cigarette use among U.S. adolescents: a cross-sectional study. JAMA Pediatr 2014; 168:610–617. [PubMed: 24604023]
4. Regan AK, Promoff G, Dube SR, Arrazola R. Electronic nicotine delivery systems: adult use and awareness of the ‘e-cigarettet in the USA. Tob Control 2013;22:19–23. [PubMed: 22034071]
5. Pearson JL, Abrams DB, Niaura RS, Richardson A, Vallone DM. Public support for mandated nicotine reduction in cigarettes. Am J Public Health 2013; 103:562–567. [PubMed: 23327262]
6. Vickerman KA, Carpenter KM, Altman T, Nash CM, Zbikowski SM. Use of electronic cigarettes among state tobacco cessation quitline callers. Nicotine Tob Res 2013;15:1787–1791. [PubMed: 23658395]
7. Lerner CA, Sundar IK, Watson RM, Elder A, Jones R, Done D, Kurtzman R, et al. Environmental health hazards of e-cigarettes and their components: Oxidants and copper in e-cigarette aerosols. Environ Pollut 2015; 198: 100–107. [PubMed: 25577651]
8. El Golli N, Dkhili H, Dallagi Y, Rahali D, Lasram M, Bini-Dhouib I, Lebret M, et al. Comparison between electronic cigarette refill liquid and nicotine on metabolic parameters in rats. Life Sci 2016;146:131–138. [PubMed: 26752340]

9. El Golli N, Jrad-Lamine A, Neffati H, Rahali D, Dallagi Y, Dkhili H, Ba N, et al. Impact of ecigarette refill liquid with or without nicotine on liver function in adult rats. Toxicol Mech Methods 2016;26:419–426. [PubMed: 27484987]
10. Moheimani RS, Bhetraratana M, Yin F, Peters KM, Gornbein J, Araujo JA, Middlekauff HR. Increased Cardiac Sympathetic Activity and Oxidative Stress in Habitual Electronic Cigarette Users: Implications for Cardiovascular Risk. JAMA Cardiol 2017;2:278–284. [PubMed: 28146259]
11. Friedman TC, Sinha-Hikim I, Parveen M, Najjar SM, Liu Y, Mangubat M, Shin CS, et al. Additive effects of nicotine and high-fat diet on hepatic steatosis in male mice. Endocrinology 2012;153:5809–5820. [PubMed: 23093702]
12. Hasan MK, Friedman TC, Sims C, Lee DL, Espinoza-Derout J, Ume A, Chalfant V, et al. alpha7-Nicotinic Acetylcholine Receptor Agonist Ameliorates Nicotine Plus High-Fat Diet-Induced Hepatic Steatosis in Male Mice by Inhibiting Oxidative Stress and Stimulating AMPK Signaling. Endocrinology 2018; 159:931–944. [PubMed: 29272360]
13. Sinha-Hikim I, Sinha-Hikim AP, Shen R, Kim HJ, French SW, Vaziri ND, Crum AC, et al. A novel cystine based antioxidant attenuates oxidative stress and hepatic steatosis in diet-induced obese mice. Exp Mol Pathol 2011;91 :419–428. [PubMed: 21570964]
14. Schierwagen R, Maybuchen L, Zimmer S, Hittatiya K, Back C, Klein S, Uschner FE, et al. Seven weeks of Western diet in apolipoprotein-E-deficient mice induce metabolic syndrome and nonalcoholic steatohepatitis with liver fibrosis. Sci Rep 2015;5:12931. [PubMed: 26263022]
15. Hamaguchi M, Kojima T, Takeda N, Nagata C, Takeda J, Sarui H, Kawahito Y, et al. Nonalcoholic fatty liver disease is a novel predictor of cardiovascular disease. World J Gastroenterol 2007;13:1579–1584. [PubMed: 17461452]
16. Lee JE, Lee YJ, Chung SY, Cho HW, Park BJ, Jung DH. Severity of nonalcoholic fatty liver disease is associated with subclinical cerebro-cardiovascular atherosclerosis risk in Korean men. PLOS One 2018; 13:e0193191. [PubMed: 29565984]
17. Shao XM, Xu B, Liang J, Xie XS, Zhu Y, Feldman JL. Nicotine delivery to rats via lung alveolar region-targeted aerosol technology produces blood pharmacokinetics resembling human smoking. Nicotine Tob Res 2013;15:1248–1258. [PubMed: 23239844]
18. Bhogal RK, Stoica CM, McGaha TL, Bona CA. Molecular aspects of regulation of collagen gene expression in fibrosis. J Clin Immunol 2005;25:592–603. [PubMed: 16380822]
19. Garcia-Carracedo D, Yu CC, Akhavan N, Fine SA, Schonleben F, Maehara N, Karg DC, et al. Smad4 loss synergizes with TGFalpha overexpression in promoting pancreatic metaplasia, PanIN development, and fibrosis. PLoS One 2015; 10:e0120851. [PubMed: 25803032]
20. Benowitz NL, Zevin S, Jacob P 3rd. Sources of variability in nicotine and cotinine levels with use of nicotine nasal spray, transdermal nicotine, and cigarette smoking. Br J Clin Pharmacol 1997;43:259–267. [PubMed: 9088580]
21. Tam NN, Gao Y, Leung YK, Ho SM. Androgenic regulation of oxidative stress in the rat prostate: involvement of NAD(P)H oxidases and antioxidant defense machinery during prostatic involution and regrowth. Am J Pathol 2003; 163:2513–2522. [PubMed: 14633623]
22. Postic C, Girard J. Contribution of de novo fatty acid synthesis to hepatic steatosis and insulin resistance: lessons from genetically engineered mice. J Clin Invest 2008; 118:829–838. [PubMed: 18317565]
23. Qin X, Xie X, Fan Y, Tian J, Guan Y, wang X, Zhu Y, et al. Peroxisome proliferator-activated receptor-delta induces insulin-induced gene-I and suppresses hepatic lipogenesis in obese diabetic mice. Hepatology 2008;48:432–441. [PubMed: 18627005]
24. Soufi N, Hall AM, Chen Z, Yoshino J, Collier SL, Mathews JC, Brunt EM, et al. Inhibiting monoacylglycerol acyltransferase 1 ameliorates hepatic metabolic abnormalities but not inflammation and injury in mice. J Biol Chem 2014;289:30177–30188. [PubMed: 25213859]
25. Matsusue K, Kusakabe T, Noguchi T, Takiguchi S, Suzuki T, Yamano S, Gonzalez FJ. Hepatic steatosis in leptin-deficient mice is promoted by the PPARgamma target gene Fsp27. Cell Metab 2008;7:302–311. [PubMed: 18396136]
26. Stacey M, Chang GW, Sanos SL, Chittenden LR, Stubbs L, Gordon S, Lin HH. EMR4, a novel epidermal growth factor (EGF)-TM7 molecule up-regulated in activated mouse macrophages,

binds to a putative cellular ligand on B lymphoma cell line A20. J Biol Chem 2002;277:29283–29293. [PubMed: 12023293]

27. Sinha-Hikim AP, Sinha-Hikim I, Friedman TC. Connection of Nicotine to Diet-Induced Obesity and Non-Alcoholic Fatty Liver Disease: Cellular and Mechanistic Insights. Front Endocrinol (Lausanne) 2017;8:23. [PubMed: 28239368]
28. Kojima H, Sakurai S, Uemura M, Fukui H, Morimoto H, Tamagawa Y. Mitochondrial abnormality and oxidative stress in nonalcoholic steatohepatitis. Alcohol Clin Exp Res 2007;31:S6166.
29. Videla LA. Cytoprotective and suicidal signaling in oxidative stress. Biological research 2010;43:363–369 [PubMed: 21249309]
30. Kudo H, Takahara T, Yata Y, Kawai K, Zhang W, Sugiyama T. Lipopolysaccharide triggered TNF-alpha-induced hepatocyte apoptosis in a murine non-alcoholic steatohepatitis model. Journal of hepatology 2009;51:168–175. [PubMed: 19446916]
31. Serviddio G, Bellanti F, Sastre J, Vendemiale G, Altomare E. Targeting mitochondria: a new promising approach for the treatment of liver diseases. Current medicinal chemistry 2010; 17:2325–2337. [PubMed: 20491641]
32. Yuan H, Shyy JY, Martins-Green M. Second-hand smoke stimulates lipid accumulation in the liver by modulating AMPK and SREBP-I. J Hepatol 2009;51 :535–547. [PubMed: 19556020]
33. Sinha-Hikim I, Friedman TC, Falz M, Chalfant V, Hasan MK, Espinoza-Derout J, Lee DL, et al. Nicotine plus a high-fat diet triggers cardiomyocyte apoptosis 2017.
34. Postic C, Girard J. Contribution of de novo fatty acid synthesis to hepatic steatosis and insulin resistance: lessons from genetically engineered mice. J Clin Invest 2008;118:829–838. [PubMed: 18317565]
35. Andersson K, Arner P. Systemic nicotine stimulates human adipose tissue lipolysis through local cholinergic and catecholaminergic receptors. International journal of obesity and related metabolic disorders : journal of the International Association for the Study of Obesity 2001 ;25:1225–1232.
36. wu Y, song P, Zhang W, Liu J, Dai X, Liu Z, Lu Q, et al. Activation of AMPKu2 in adipocytes is essential for nicotine-induced insulin resistance in vivo. Nat Med 2015;21 :373–382. [PubMed: 25799226]
37. Liu RH, Mizuta M, Matsukura S. The expression and functional role of nicotinic acetylcholine receptors in rat adipocytes. J Pharmacol Exp Ther 2004;310:52–48. [PubMed: 14993259]
38. Jacobi D, Liu S, Burkewitz K, Kory N, Knudsen NH, Alexander RK, Unluturk U, et al. Hepatic Bmall Regulates Rhythmic Mitochondrial Dynamics and Promotes Metabolic Fitnsess. Cell Metab 2015;22:709–720. [PubMed: 26365180]
39. Shimba S, Ogawa T, Hitosugi S, Ichihashi Y, Nakadaira Y, Kobayashi M, Tezuka M, et al. Deficient of a clock gene, brain and muscle Arnt-like protein-I (BMALI), induces dyslipidemia and ectopic fat formation. PLoS One 2011 ;6:e25231. [PubMed: 21966465]
40. O'Neil D, Mendez-Figueroa H, Mistretta TA, Su C, Lane RH, Aagaard KM. Dysregulation of Npas2 leads to altered metabolic pathways in a murine knockout model. Mol Genet Metab 2013;110:378–387. [PubMed: 24067359]
41. Lee SM, Zhang Y, Tsuchiya H, Smalling R, Jetten AM, Wang L. Small heterodimer partner/ neuronal PAS domain protein 2 axis regulates the oscillation of liver lipid metabolism. Hepatology :497–505.
42. Zhou P, Ross RA, Pywell CM, Liangpunsakul S, Duffield GE. Disturbances in the murine hepatic circadian clock in alcohol-induced hepatic steatosis. Sci Rep 2014;4:3725. [PubMed: 24430730]
43. Benowitz NL, Hukkanen J, Jacob P 3rd. Nicotine chemistry, metabolism, kinetics and biomarkers. Handb Exp Pharmacol 2009:29–60. [PubMed: 19184645]
44. Hukkanen J, Jacob P 3rd, Benowitz NL. Metabolism and disposition kinetics of nicotine. Pharmacol Rev 2005;57:79–115. [PubMed: 15734728]

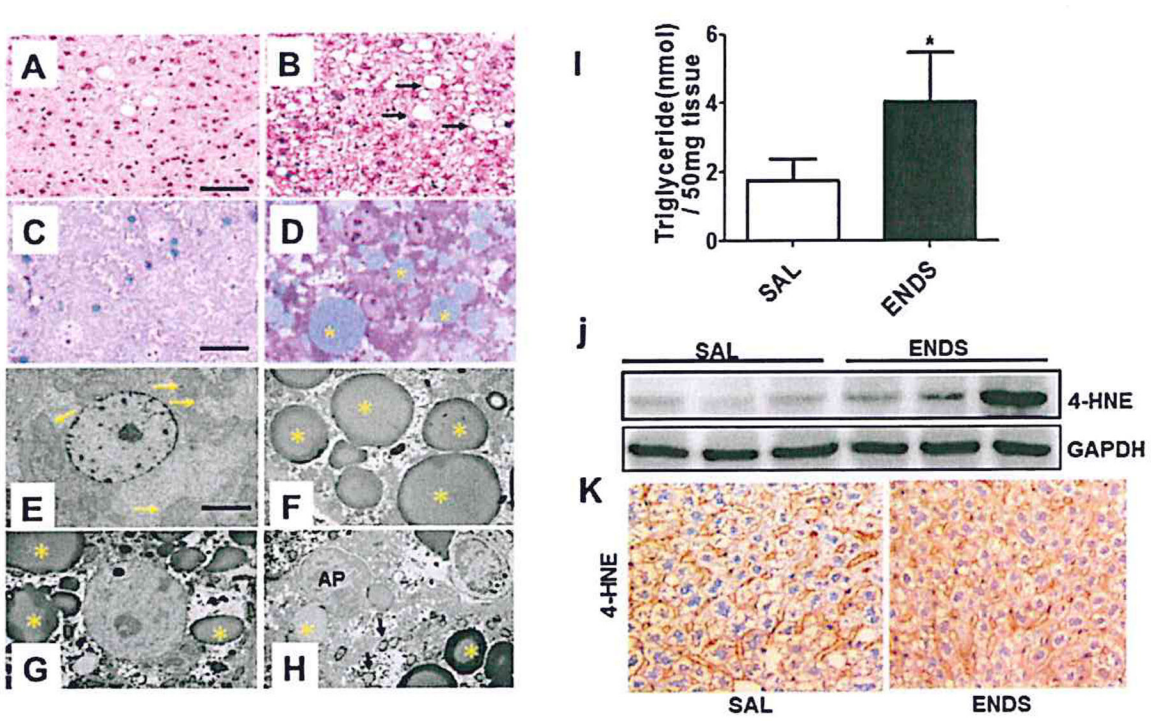


**FIG. 1.**

H&E stained liver sections show increased lipid accumulation (black arrow) in ApoE−/− mice exposed to ENDS (B) compared to ApoE−/− mice exposed to saline (A). Light microscopic images of glutaraldehyde-fixed, osmium tetroxide-post-fixed, epoxy embedded, and toluidine blue stained liver sections form saline (C) and ENDS-treated mice (D) show a striking increase in lipid accumulation (yellow asterisks) of varying sizes in ENDS-treated mice (D). Representative TEM images from control (E) and ENDS exposed livers (F-H) show a striking increase in lipid accumulation of varying sizes (yellow asterisks) along with a decrease in the intracellular organelles in hepatocytes in ENDS exposed livers. Also shown in Fig. 1H, is an apoptotic hepatocyte nucleus (AP) and many vacuolated mitochondria (black arrow). (I) Hepatic triglyceride levels in saline (SAL) and ENDS exposed mice. * P<O.05. (J) Western blot analysis shows increased hepatic 4-HNE levels in ENDS exposed mice. GAPDH in the immunoblot is shown as a loading control. (K) Changes in the in vivo patters of 4-HNE expression between saline and ENDS treated livers. Scale bar=25 μm for A–D and 1 μm for E–H.

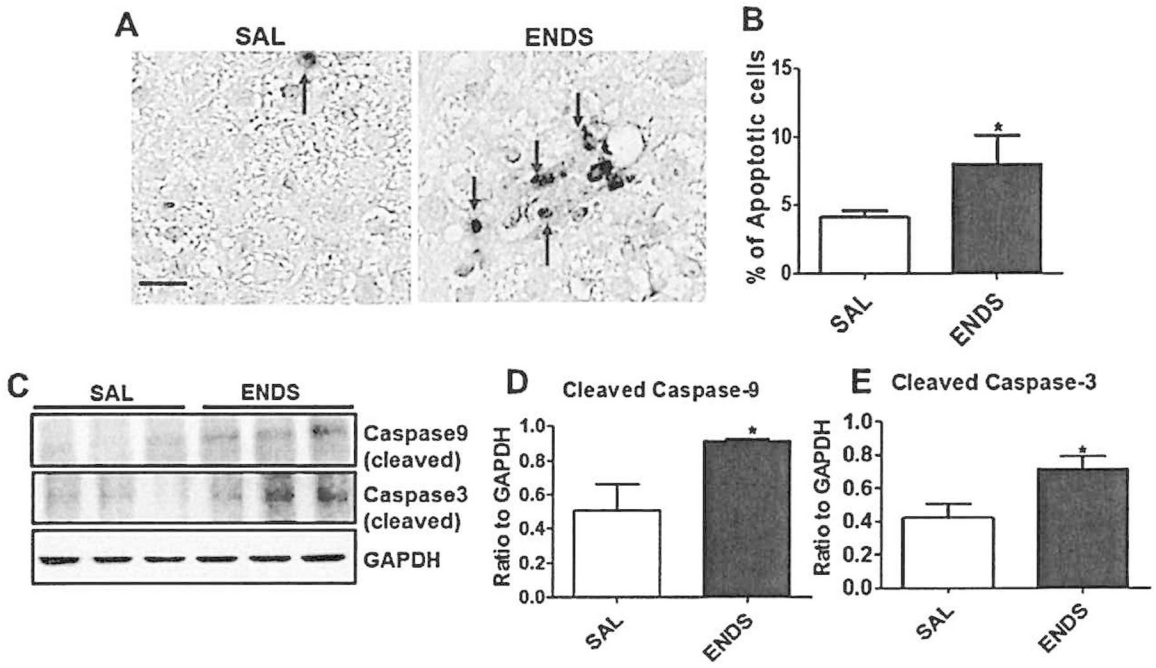


**FIG. 2.**

In situ detection of hepatocyte apoptosis by TUNEL (A). (B) Quantitation of apoptosis. * P<O.05. (C) Western blot analysis shows increased expression of both cleaved (active) caspase 9 and 3 in ENDS-treated liver. (D, E) Quantitation of band intensities. Data for active caspase 9 and 3 were normalized to GAPDH. * P<0.05.

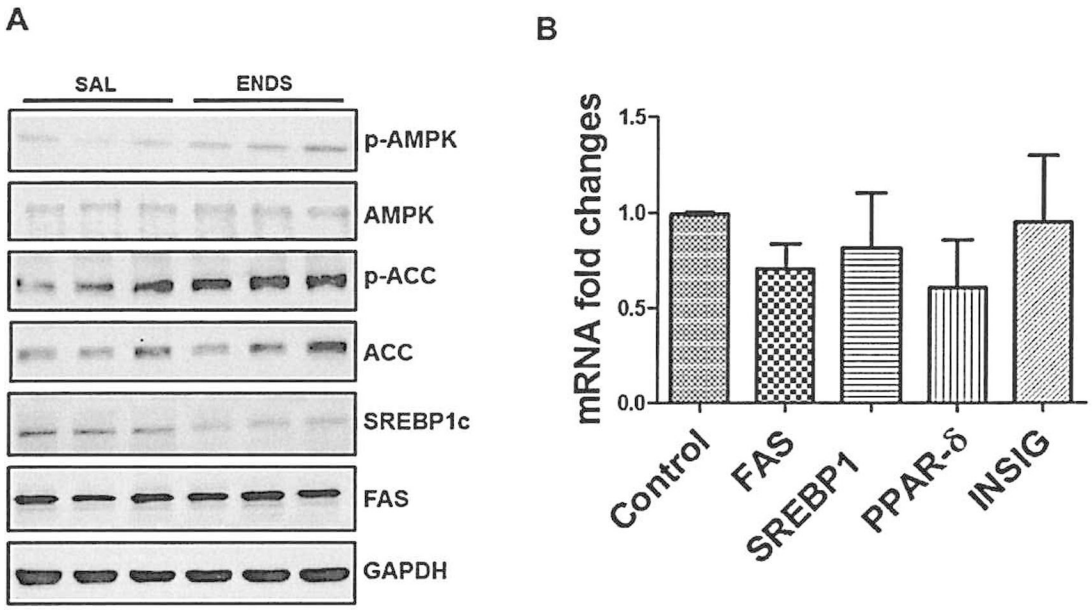


**FIG. 3.**

(A) Western blot analysis of hepatic expression of phospho-AMPK (p-AMPK), total AMPK, phospho-ACC (p-ACC), total ACC, SREBP1c, and FAS between saline and ENDS exposed mice. (B) Quantitative RT-PCR analysis of hepatic expression of SREBP1c, FAS, PPARδ, and INSIG1 between saline and ENDS exposed livers.

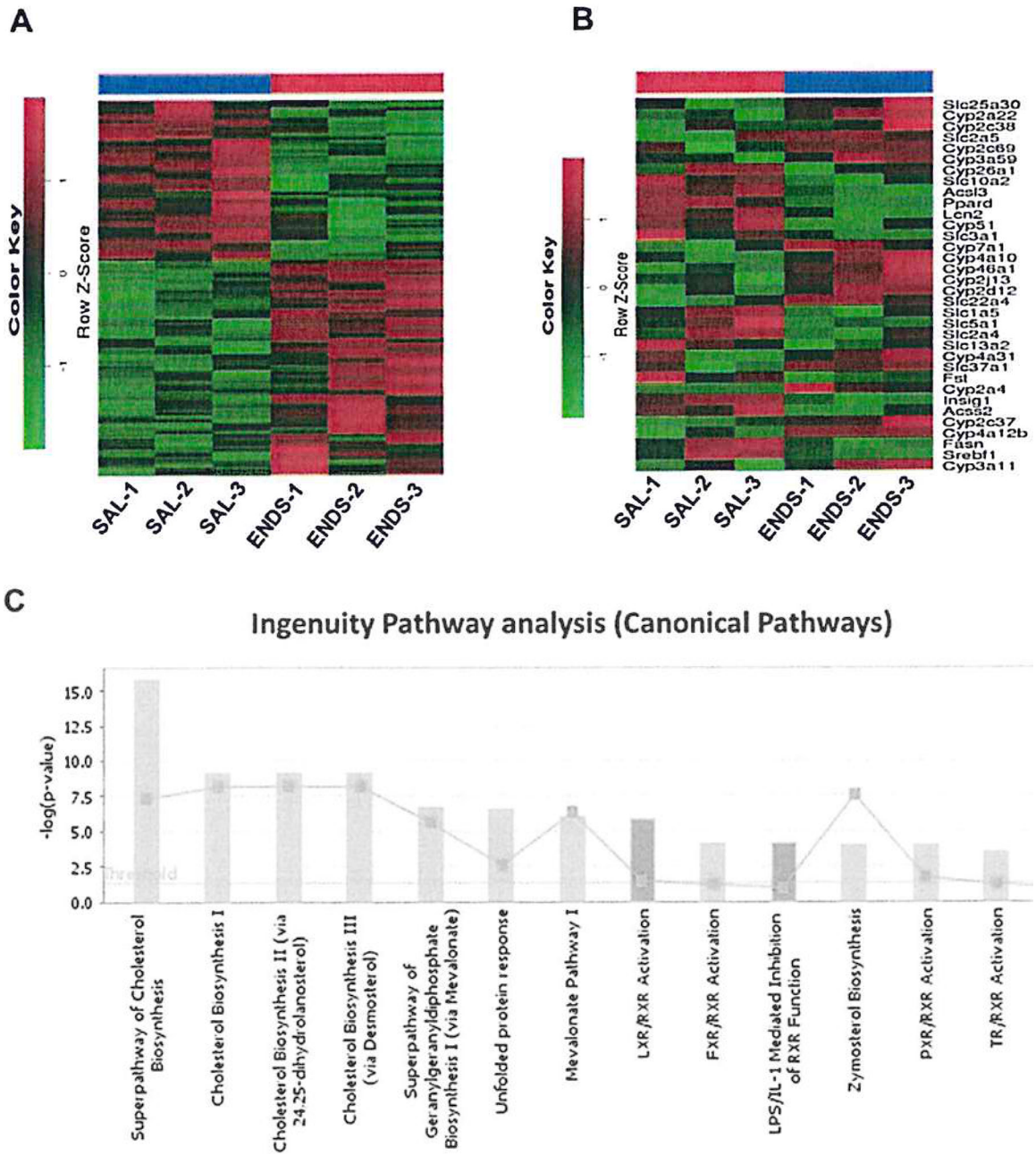

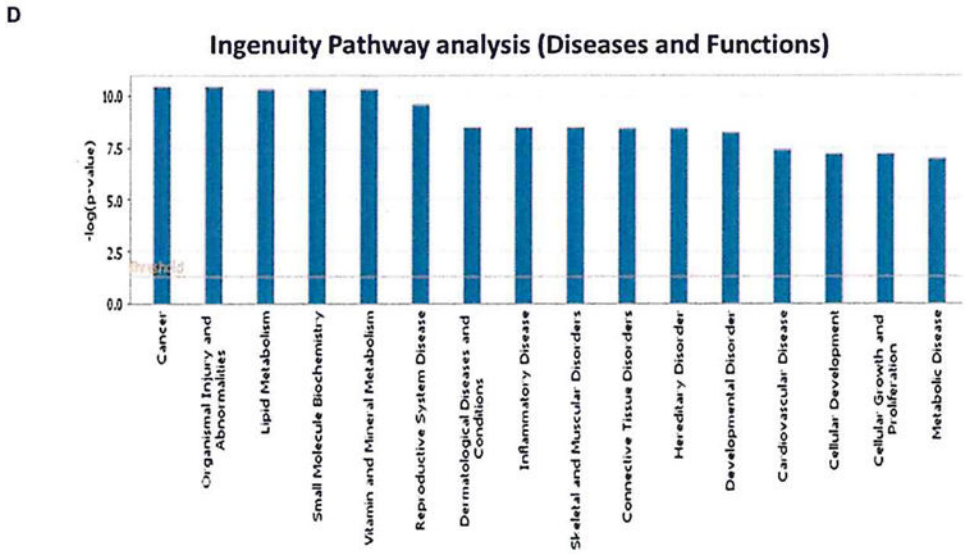


**FIG. 4.**

(A) Two-dimensional hierarchical clustering of 433 differentially (P<0.05) expressed genes. (B) The columns of the heat map represent 34 differentially expressed genes. The RNA-seq analysis using IPA software reveals canonical pathways (C) and diseases (D) are most strongly associated with the differentially expressed genes. The P value is assigned based on the likelihood of obtaining the observed number of signaling pathway or disease-related gene in a given data set by chance alone. (Grey bar= either activated or inhibited not predicated due to lack of enough information in IPA knowledge base, Blue bar= the pathways are downregulated)

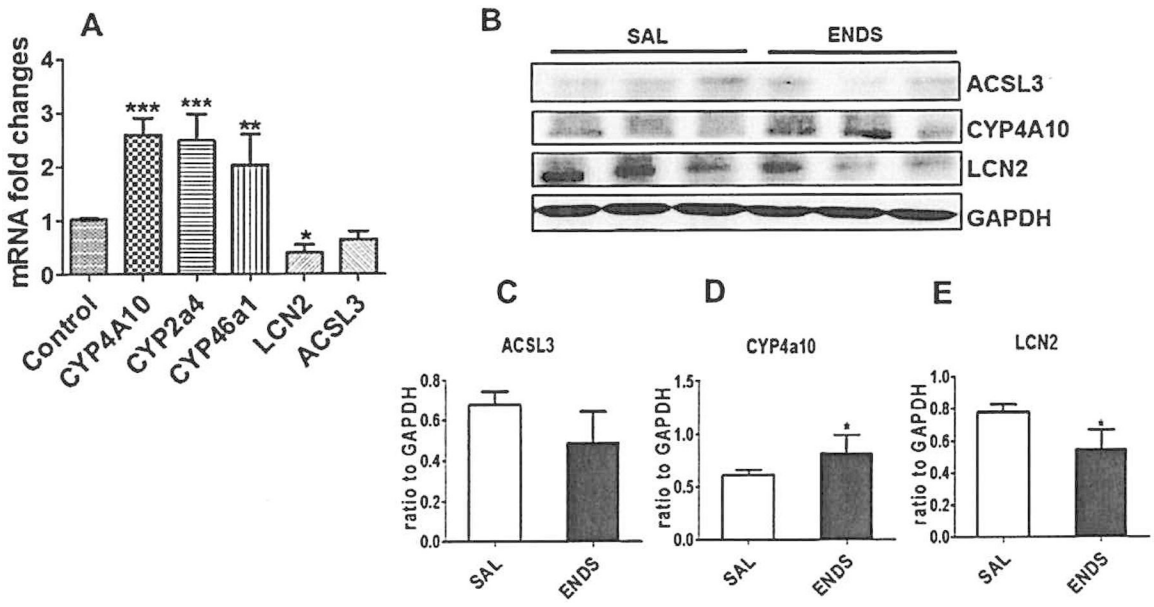


**FIG. 5.**

(A) Quantitative RT-PCR data reveal significant up-regulation of Cyp4A10, Cyp2A4, and Cyp46 Al and a significant down-regulation of LCN2 with no change in the expression of ACSL3. Values are means ± SEM (n=6). (B) Western blot analysis validates the results obtained by q-RT-PCR. (C-E) Quantitation of band intensities. Values are normalized to GAPDH. * P < 0.05, **P<0.01, ***p<001.

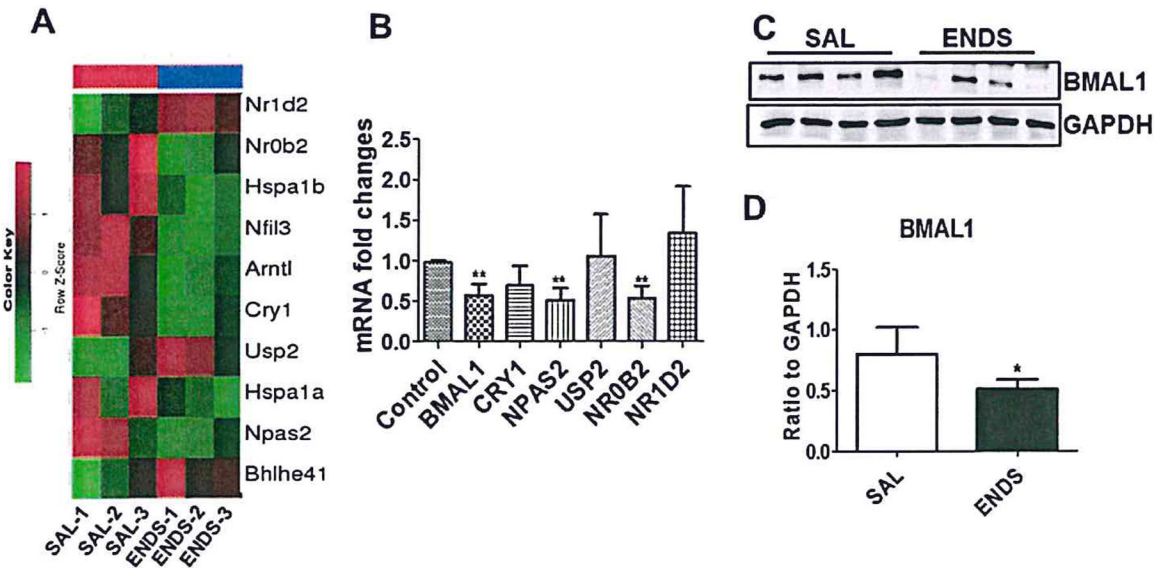


**FIG. 6.**

(A) The columns of the heat map represent 10 differentially expressed genes. (B) Quantitative RT-PCR analysis shows down regulation of three prominent genes of the hepatic circadian core system, including BMAL1, NPAS2, and NR0B2 in ENDS-treated livers compared with saline-exposed livers. $P < 0.05$. Hepatic down-regulation of BMAL1 is further substantiated by western blot analysis (C). (D) Quantitation of band intensities. *$P < 0.05$.

**Table-1:**

Changes in the expression of genes associated with lipid storage, droplet formation and inflammation.

| Genes | Name | RNA seq | | RT-PCR | |
|---|---|---|---|---|---|
| | | Fold chanes | P-value | Fold chanes | P-value |
| CIDEA | cell death-inducing DNA fragmentation factor, alpha subunit-like effector A | 1.61 | .000507 | 3.077 | .0169 |
| CIDEC | cell death-inducing DFFA-like effector c | 2.45 | .000068 | 2.572 | .0656 |
| MOGAT1 | monoacylglycerol O-acltransferase 1 | 2.05 | .000754 | 2.175 | .0666 |
| EMR1 | EGF-like module-containing mucin-like hormone receptor-like 1 F4/80 like protein | 1.15 | .392357 | 0.961 | .4551 |
| EMR4 | EGF-like module-containing mucin-like hormone receptor-like 4 (F4/80 like protein) | 1.76 | .001402 | 1.729 | .0071 |